# Progress in Understanding the Combustion Physics for Hypergolic Propellants

Stephen D. Heister & Timothée L. Pourpoint
*Purdue University, West Lafayette, IN, 47907*

## Abstract

In 2008, a team led by Purdue University was granted a contract from the U.S. Army Research Office under the Multidisciplinary University Research Initiative (MURI) program to study combustion of gelled hypergolic propellants. A team led by Penn State University was also awarded a MURI on this same topic. As a result, the past five years have seen some intense research activity in the U.S. research community in the hypergolic combustion area. This paper summarizes some current work in liquid and gas-phase combustion kinetics, in droplet collisions, and in resolving the thin gas layer formed between impinging jets.

## 1. Introduction

Since the earliest days of rocket development in the WWII era, the advantages of hypergolic propellant combinations have been well recognized. Because rockets are by their very nature high-flow devices, ignition is always a challenging prospect. Any pooling of uncombusted propellants in the chamber prior to the ignition event can lead to hard starts and hardware damage. The spontaneous combustion afforded by hypergolic propellant combinations provides for restartability and pulsed operations, which are essential for a number of applications.

Most flight applications of hypergolic engines employ oxidizers based on nitric acid (e.g., IRFNA, WFNA, MON, and NTO). Hypergolic fuels for these engines used furfural alcohol (in early engines), but hydrazine, and its derivatives MMH and UDMH, have supplanted it in modern applications. Although much less studied, hydrogen peroxide is highly hypergolic with a number of catalyst materials such as potassium permanganate, manganese dioxide, and sodium borohydride [1]. In the present work, we focus on IRFNA/WFNA and MMH combinations.

It is challenging to gain fundamental knowledge of the processes in hypergolic combustion because it is impossible to distinguish between chemistry and fluid mechanics in these violent and highly transient ignition events. Early work was largely empirical: a variety of screening tools such as drop tests or impingement tests [2] were used to assess ignitability and the influence of propellant composition and operating conditions on the ignition behavior. Lacking high speed computational power, researchers developed quasi-analytic treatments to investigate droplet evaporation, mixing, and ignition processes with a goal of providing a design capability [3]. High-speed film cameras provided some glimpse of the millisecond time-scale events [2]. Here we focus on recent knowledge gained from modern tools; the interested reader is referred to reviews of the classic literature [4].

The ever-increasing capability of modern high-speed cameras and other diagnostics, combined with improving computational power, has allowed significant advancements in the understanding of hypergolic combustion physics. While the kinetics associated with the nitric acid/hydrazine system are daunting, computational tools are now progressing with reaction sets including over 500 intermediate reactions. Recent observations with high speed cameras and other instrumentation have provided an understanding of microsecond-level events and helped uncover the role of liquid phase and droplet atomization/explosion processes revealing micron-scale features not observed with prior tools. The observation of micron-scale gas layers between sheets of impinging liquids has provided another area of study. As a result of these advances, our current view of the hypergolic ignition/combustion event has evolved to include these new focus areas.

These areas (kinetics behavior, droplet explosions, gas films, liquid phase reactions) serve as the prime topics of discussion in the present work. Figure 1 provides an overview of these processes for a classical impinging jet arrangement used in many hypergolic engines. The confluence of the high speed liquid jets creates a prominent egg-

shaped sheet that extends downstream of the impingement region. Impact waves are large scale structures that form in the impact region and convect downstream, ultimately breaking into ligaments and, in turn, into droplets that generate the resulting spray. These features are well known and have been studied previously [5], but their exact origin is still in debate. Current theories point to instability of the stagnation point formed at the center of the impact or hydrodynamic instabilities fed from the injectors themselves.

A less-discussed feature, highlighted in Fig. 1, is a very thin gas layer that separates the two propellants as they form the respective undulating fuel and oxidizer sheets. To our knowledge this feature (which is exaggerated for clarity in Fig. 1) has never been imaged, although we theorize that it must be present because the two liquids cannot lie directly adjacent to each other without producing large amounts of gases. We know from early experimental concepts aimed at studying hypergolic ignition that coaxial arrangements were discarded as mixing was poor, probably because a gas layer separated the two propellants.

The formation of this gas layer is the subject of our recent study. In the impact region, highly unsteady and spatially-distributed gas evolution occurs primarily due to Rayleigh-Taylor instability. Recent studies provide important information about the rate of gas generation, and the composition of gases formed from these liquid phase reactions. While the gases evolved from the reaction are quite hot (as discussed below), there is tremendous quenching potential in the latent heat of the cold liquids convecting into the region. We can imagine this layer separating the propellants (perhaps with intermittent interruptions due to hydrodynamic instabilities) as they form sheets which become thinner as they move downstream. This barrier can support a significant velocity difference between the two fluids. The differing densities of the two fluids typically dictates that they be injected at different velocities to cancel transverse momentum at the impact point. For this reason, the two sheets could expand at different rates, but large viscous forces would presumably act to remove this velocity difference as the sheet expands and moves downstream.

Droplets emanating from the impact region are subject to differential deceleration dependent on their initial diameter and provide a mechanism for collisions within dense regions of the spray. Recent high resolution visualizations and droplet investigations reveal the potential for individual ignition points to be generated from events of this nature.

Finally, the differing vapor pressure in the fluids provides for variations in gas phase stoichiometry throughout the spray and thus can affect the local ignitability of the mixture. It is this detailed picture of the events that is unfolding as a result of our work. The next sections of this paper provide evidence supporting the sequence of events described here as well as a quantitative basis for advanced models of the entire two-phase ignition process.

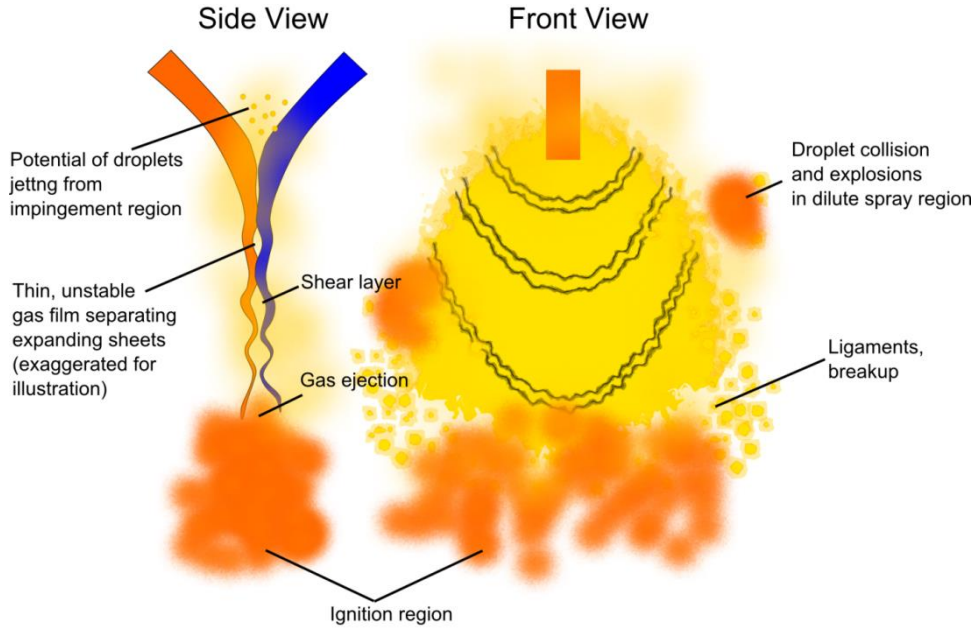


Figure 1: Schematic of impinging jet hypergolic ignition highlighting important physical processes

## 2. Progress in Combustion Kinetics

Between 2003 and 2005, the U.S. Army Research Lab embarked on development of a full mechanism for IRFNA/MMH kinetics. This dataset [6], which involves over 81 intermediate species and 513 individual reactions, is arguably the most comprehensive set available at present. Groups sponsored by a recent Multidisciplinary University Research Initiative sponsored by the Army Research Office have been developing reduced order mechanisms for this reaction with the hope of streamlining CFD-based combustion computations using these kinetics models. One of the interesting and troubling outcomes from these investigations is that the gas-phase kinetics models will not support ignition unless the initial mixture is at significantly elevated temperatures (in the range of 600-800K depending on the mechanism employed) [7]. Recent work by Smith [8] and Thynell [9] have helped to illuminate this inconsistency using high speed diagnostics to assess liquid phase acid/base reactions that provide an initial condition for gas-phase kinetics. We suggest that the pertinent reaction of principal importance is:

$$2HNO_3+CH_3N_2H_3 \rightarrow CH_3ONO_2+2.5H_2O+0.5N_2O+N_2 \quad (1)$$

This reaction produces methyl nitrate (additional fuel supply), nitrous oxide (additional oxidizer), and the final combustion species, water vapor and nitrogen. The reaction produces an adiabatic flame temperature of 1209 K, thereby providing sufficient energy to bootstrap gas-phase kinetics processes. Labbe and Westmoreland [10] developed a gas-phase reduced mechanism that uses species formed in the liquid phase reactions. This mechanism serves as the current basis for study in our group. Figure 2 shows zero-dimensional calculations using this 41 species, 200 reaction mechanism. The results in Fig. 2 assume an initial mixture temperature of 600 K, which is well below the adiabatic flame temperature for the liquid phase reaction in Eq. 1. An inflection is evident for cases that successfully ignite. This characteristic is caused by endothermic decomposition reactions of fuel species. Stoichiometric or slightly fuel lean conditions provide the most favorable environment for ignition. Historically, engines using this propellant combination have used an oxidizer lead in order to better support ignition. These new detailed chemical kinetics computations reinforce the desirability of having oxidizer-rich regions.

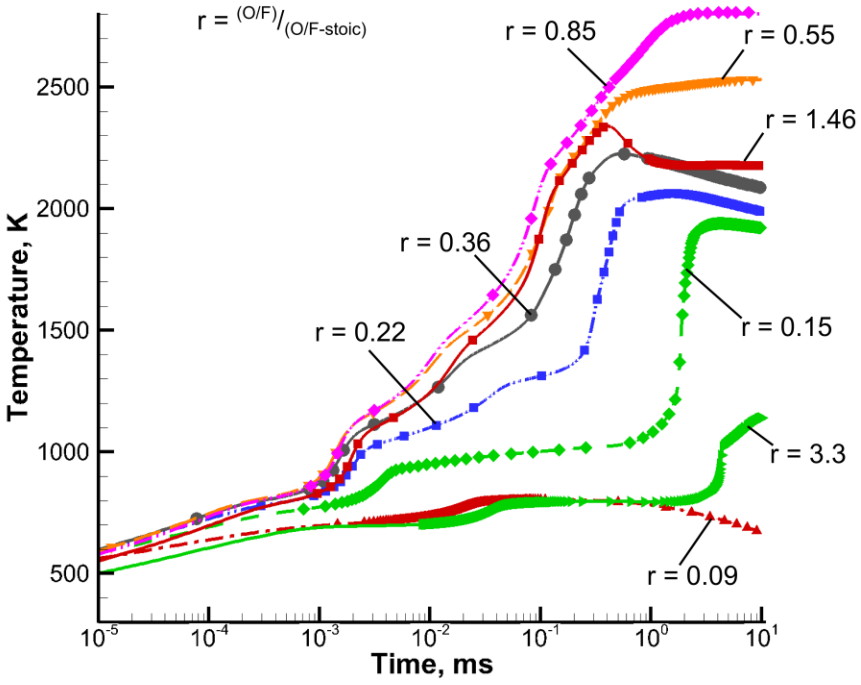


Figure 2: Ignition characteristics [7] of WFNA/MMH mixtures employing reduced order mechanism of Labbe and Westmoreland [10]. Computations assume an initial mixture temperature of 600 K.

Figure 3 provides an additional perspective on this point. It shows ignition delays vs. O/F ratio for a variety of initial gas temperatures. The ignition delay becomes largely independent of stoichiometry for high O/F conditions, while it increases sharply for fuel rich conditions. Additionally, empirically-observed ignition delays of the order of a few milliseconds can be replicated assuming the gas mixture is initially between 550 and 650 K. Since the liquid phase reactions provide temperatures as high as 1200 K, there are ample opportunities to generate these conditions within a

spray. At the full adiabatic flame temperature of the liquid phase reaction, ignition times would be measured in microseconds. This result may provide an important connection to explanation of drop impact physics as discussed in the next section.

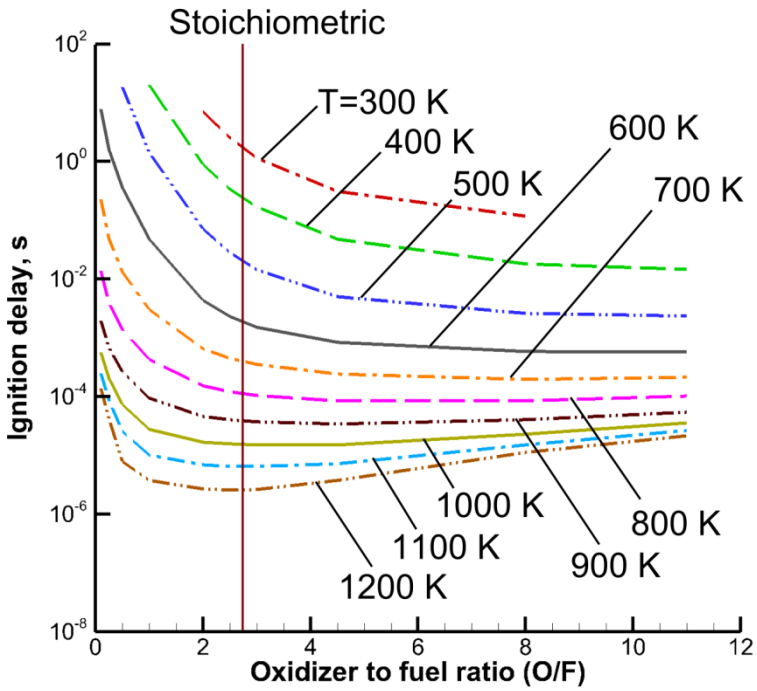


Figure 3: Ignition delay characteristics of WFNA/MMH mixtures for various initial mixture temperatures.

## 3. Modeling Jet Impingement using Liquid Phase Reactions

The detailed evolution of flow processes within the impingement region continues to be elusive. Experimentally, it is challenging to observe this region because it can become obscured by droplets or by complex undulations of the free surfaces of the two jets. To our knowledge, gas evolution between the jets has never been imaged. Hydrodynamically, the gases formed from liquid/liquid impact are supporting the full stagnation pressure of the impact zone and therefore the region will be subject to powerful Rayleigh-Taylor instabilities as the lighter gases attempt to support the heavier, decelerating liquids. Computationally, this region is equally challenging because two-phase processes and very rapid kinetics play dominant roles. Time scales relevant to this tiny region are typically measured in microseconds, so the extent to which fluid evaporation plays a role in cooling gases produced by liquid phase reactions is difficult to assess. Finally, a complete reaction rate set for the liquid phase kinetics processes is lacking. Given these challenges, it is not surprising that this particular problem has not yet received substantial attention from the research community.

Our recent modeling efforts have focused on the treatment of gas evolution and heat transfer for directly-opposed impinging jets. Companion 3-D computations are also in work, but the mesh sizes and run times for these computations make for slow progress. We derived a frequency factor for the Arrhenius expression for the liquid phase reactions from considerations in Fig. 4, which plots the temperature response of a global reaction mechanism assuming an activation energy of zero. An $A$ value of $10^{16}$ 1/s was selected to provide times consistent with observed gas evolution upon liquid/liquid contact (see next section for discussion).

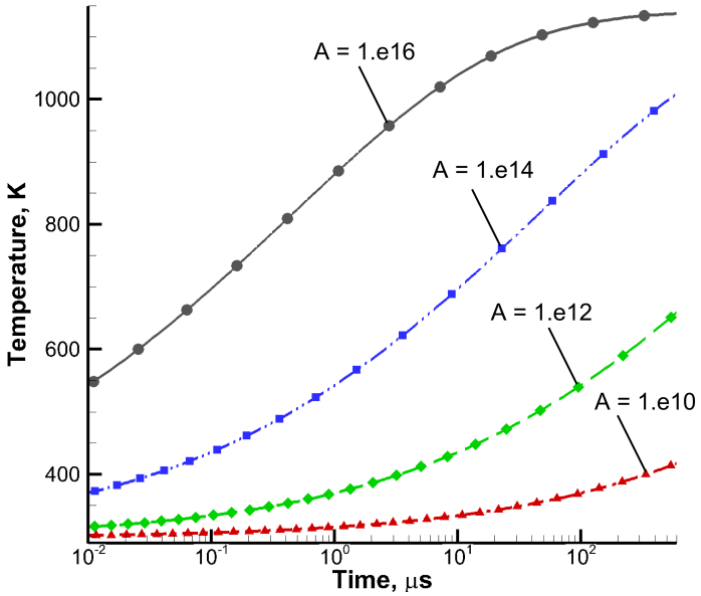


Figure 4: Arrhenius rate constant/frequency vs. temperature assuming a single step reaction with activation energy of zero.

We used the Langmuir's model to model vaporization of liquids subjected to hot gases formed from liquid phase reactions.

$$\dot{m} = \frac{Sp_{vref}}{\sqrt{2\pi MR}} \frac{1}{\sqrt{T}} e^{\frac{\Delta H_v}{2.303R}\left(\frac{1}{T_{ref}} - \frac{1}{T}\right)} \tag{2}$$

Here, $\Delta H_v$ is heat of vaporization, $M$ is molecular weight, $R$ is the universal gas constant and $Sp_{vref}$ is the specific heat of the vapor at reference temperature $T_{ref}$. Average values for the heats of vaporization of the fuel and oxidizer were used. The liquid phase reactions are presumed to occur instantaneously upon contact. Recent droplet testing indicates a delay of about 20 μs. Unfortunately, events in the impingement region occur much faster than 20 μs, so additional modeling fidelity will likely be required to completely resolve this issue.

Figure 5 provides a time history detailing the simulated flow field evolution in the impingement region. It shows alternate collapse and generation of the gas film via the Rayleigh-Taylor instability. Collapse/reformation events occur on a time scale of a few hundred μs.

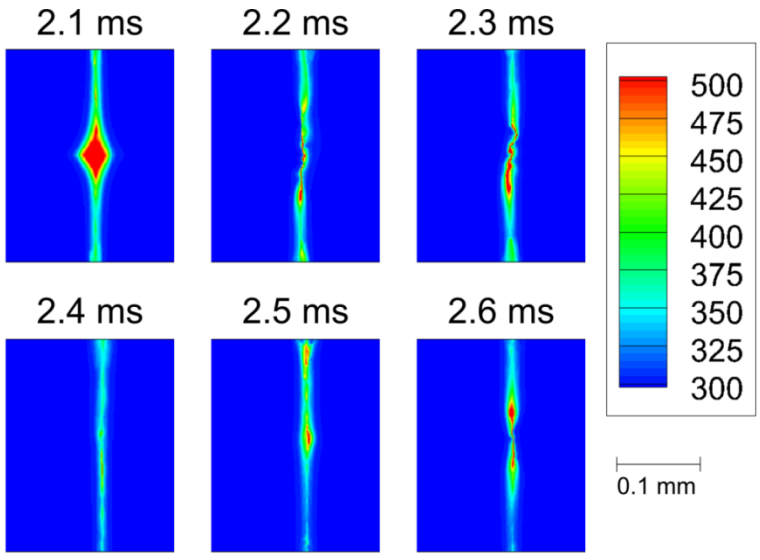


Figure 5: Sequence of images of impact region for directly opposed WFNA/MMH jets showing unsteady gas evolution near the stagnation point.

The mixture composition and gas temperature along the centerline of the impact cylinders are shown in Fig. 6 for mesh sizes of one and two microns. While both cases show similar behavior, additional structure is revealed in the finer mesh. The peak temperature, reached at the center of the impact zone, is ~430 K for both meshes, indicating that the large heat sink in the liquids near the gas boundary quenches reactions under the simulated conditions. The popping phenomenon has long been discussed in the hypergol literature and the present calculation provides some new insight. If the liquid jets approach at lower velocities, less quenching may occur in the impact region, thereby permitting gas-phase kinetics to become active, providing potential for vigorous energy release that may temporarily blow jets apart.

Finally, we note in Fig. 6 that the average thickness of the gas layer is of the order of 40 μm. If indeed this thickness could be determined experimentally it would be quite an achievement.

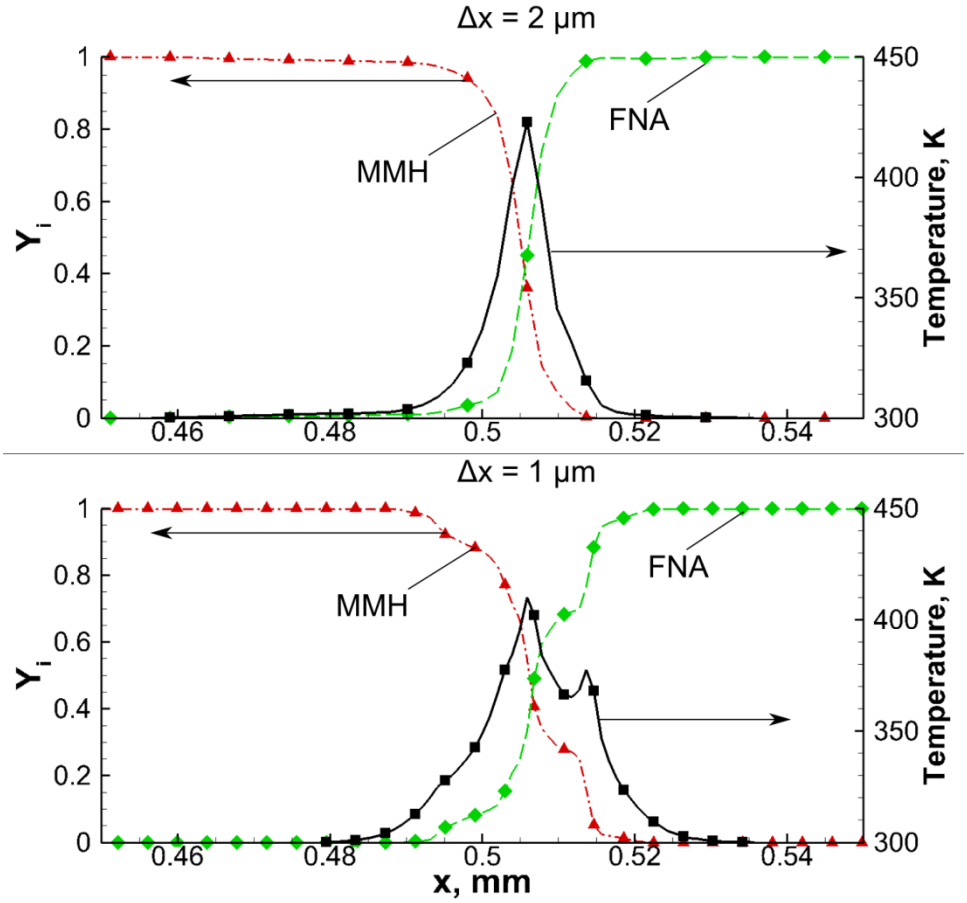


Figure 6: Time-averaged concentrations of fuel/oxidizer and gas temperature along the centerline of the impact plane.

## 4. Droplet Collisions and their Role in Ignition

The increased bandwidth and resolution of high speed cameras is providing a glimpse of more and more detailed processes stemming from hypergolic droplet collisions. Figure 7 provides an excellent representation wherein an individual droplet collision outcome was observed in the spray region of an atmospheric pressure impinging jet experiment. As illustrated in Figure 7, collision and partial mixing of dissimilar drops leads to a propulsive behavior and eventual ignition for the larger drop.

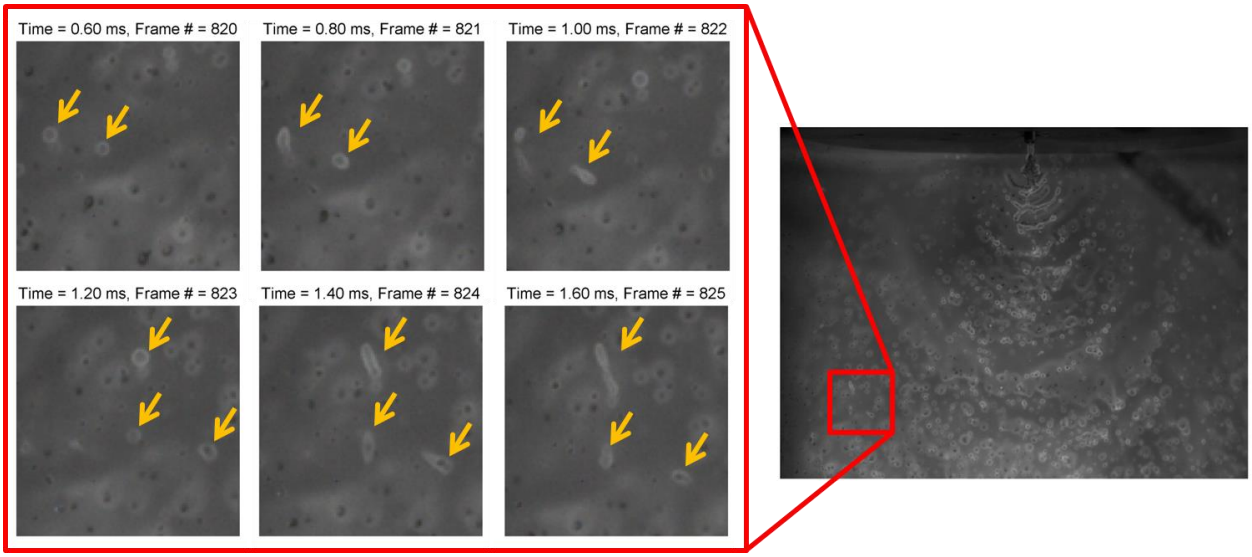


Figure 7: Drop collision and ignition event in dilute spray region within impinging jet combustion site (MMH/RFNA, Fuel injection velocity = 7 m/s, Oxidizer injection velocity = 5.8 m/s, O/F = 2).

The outcomes from drop collision events are highly complex and parameters known to influence behavior of non-reacting drops include:

- Weber number based on relative velocity of collision, $We = \frac{\rho v^2 d}{\sigma}$,
- Splashing parameter, $E^2 = \frac{We}{min\left(\frac{h_0}{d},1\right)+1/\sqrt{Re}}$, where $Re = \frac{\rho v d}{\mu}$ is the Reynolds number based on relative velocity of collision,
- Impact angle (as measured between a droplet impacting a pool),
- Impact parameter, *B*, where an impact parameter of 0 corresponds to a head-on collision and 1 corresponds to a glancing collision.

Outcomes from collisions include the potential for merging/coalescence, bouncing, or splashing. A classical representation of these regimes (for non-reacting drops impacting a pool) is shown in Fig. 8, which shows the complex topology that defines outcomes of collision events. The droplet shape at the time of collision (which may not be perfectly spherical) is another parameter that has yet to be studied purposefully. Presumably vibration of the drop to prolate/oblate shapes during its fall toward the pool lends a stochastic nature to the observed trends.

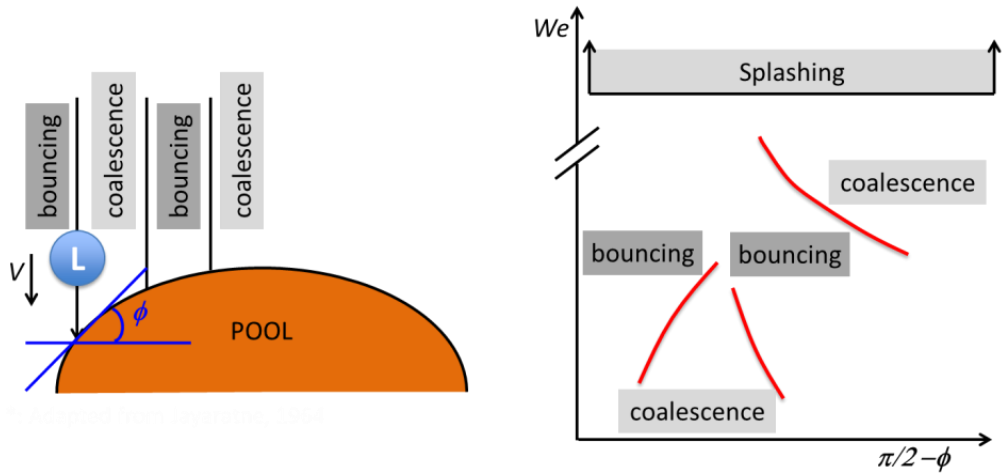


Figure 8: Classification of nonreacting drops impacting a pool (Adapted from [11])

For hypergolic drops, gas evolution and energy release provide for additional physics. The heat of combustion/reaction and ignition delay (induction time) become other highly relevant parameters determining the outcome from a collision event. The temperature of the drops also presumably plays a significant role, but this parameter has been studied very little in the community. The high vapor pressure of the oxidizers makes it difficult to investigate higher temperatures as the fluid tends to vaporize at atmospheric pressure.

Classification from recent drop tests provides evidence of bouncing, splashing and "popping" or "explosive" events. Coalescence really does not appear to occur in these reactive cases since the drop will either be ejected from the pool due to gas buildup between the two fluids, or an explosive, popping event results. Figure 9 provides a sequence of images from a bouncing event. There is sufficient gas production (and insufficient drop momentum) to support the weight of the droplet via the Leidenfrost effect. Gases do escape from the periphery of the affected area, but at a rather modest rate in comparison to the other regimes. In some cases, the droplet bouncing is visible in the imagery, but more often than not the droplet is obscured by gases being ejected at the edge of the contact surface between the two fluids.

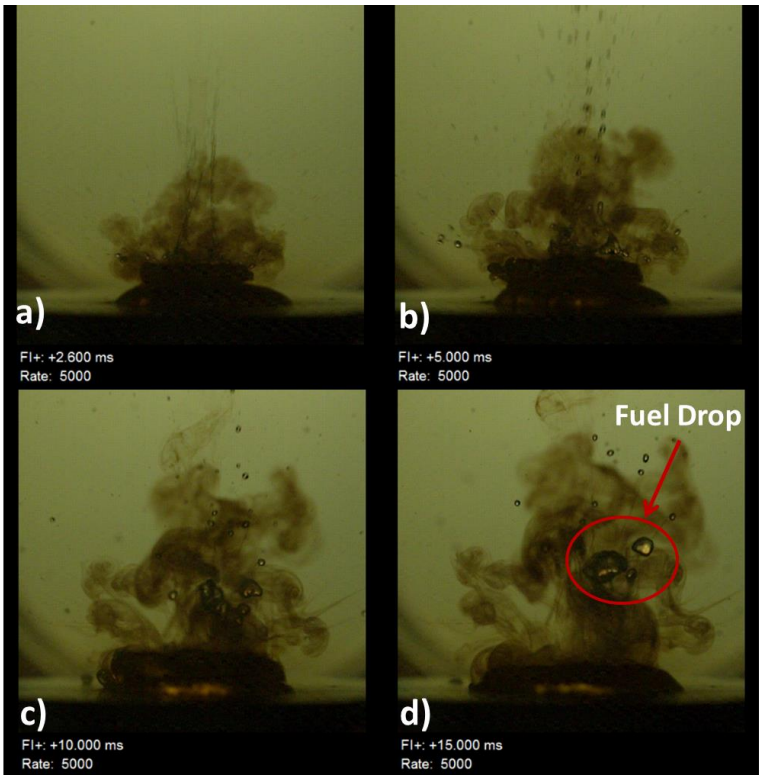


Figure 9: Sequence of images leading to a drop of MMH bouncing out of a pool of RFNA. d = 2.3 mm, v = 1.3 m/s, We = 99, (E = 11.4), pool volume = 60 μL. All times are referenced to contact.

Figure 10 provides a sequence of events for a collision classified as "splashing". There is sufficient kinetic energy of collision to create smaller droplets and ligaments that are shed from the pool. There is minimal gas production in these collisions; most of the features expanding from the pool appear to be ligaments of the two liquids.

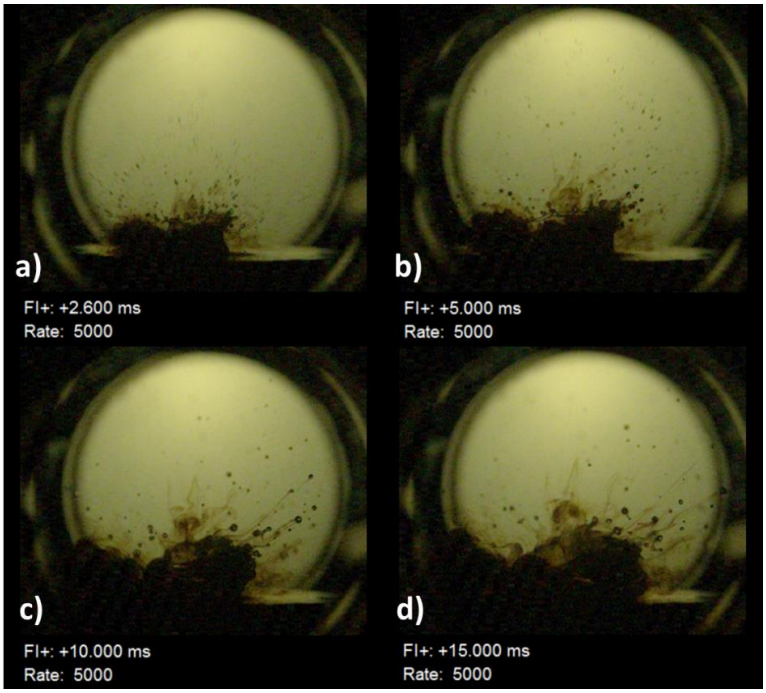


Figure 10: Sequence of images leading to a drop of MMH impacting a pool of WFNA resulting in a splash. d = 2.4 mm, v = 2.85 m/s, We = 501, E = 26.0, pool volume = 40 μL. All times are referenced to contact.

We believe that the popping events are the result of an induction period wherein gases evolved between the droplet and pool remain trapped and presumably heat to the ignition temperature with an explosive outcome. Figure 11 provides a series of images of a popping event to give readers an appreciation of the violent nature of the reaction. Recent results of Dambach [12] and Forness [2] provide a significant database of outcomes from dozens of drops over a range of velocities/Weber numbers and impact angles/parameters. The outcomes of the events seem to correlate best with Weber number, although much scatter remains due to the highly stochastic nature of the events.

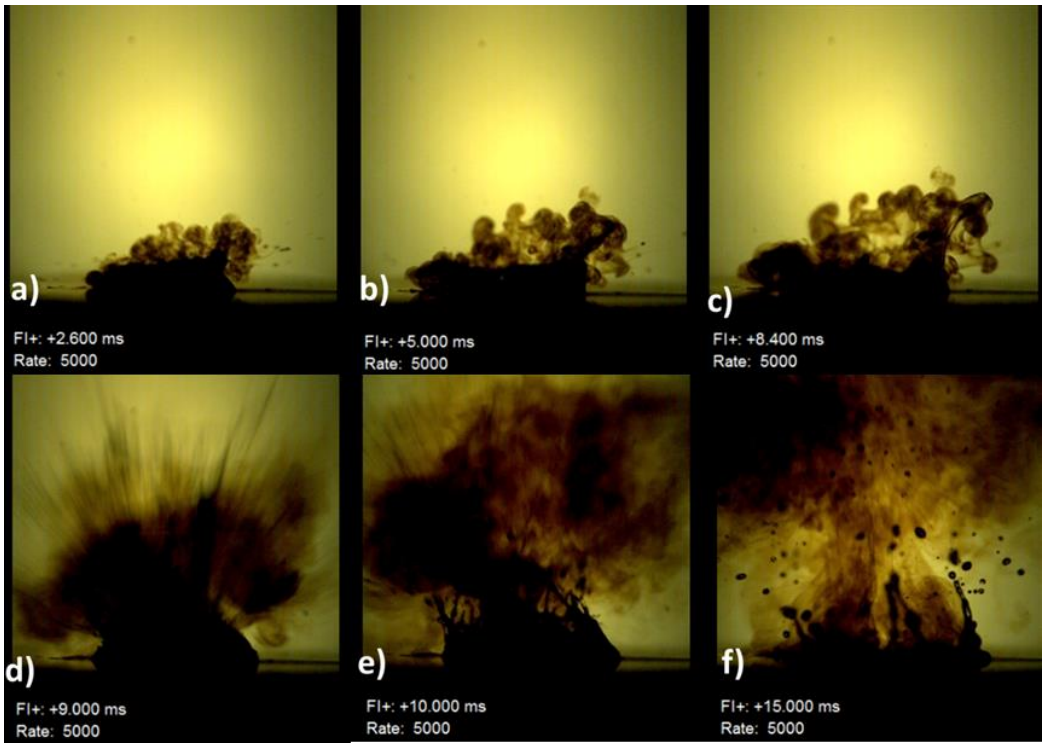


Figure 11: Sequence of Images from a MMH/WFNA explosion impact. d= 2.4 mm, v = 1.3 m/s, We = 100, pool volume = 50 μL, E = 14. All times are referenced to contact.

Figure 12 summarizes the classification of these drop/pool collisions. Choosing impact angle, impact parameter, or O/F leads to similar outcomes with groupings of classifications centered solely on the Weber number. Bounce and popping events characteristically occur at lower Weber numbers, whereas higher Weber collisions lead to splashing. The regimes are consistent with experimental inferences of popping phenomena in real engines; lower energy collisions provide sufficient residence time for gas phase kinetics to proceed and lead to explosive increases in gas volume. Considering Fig. 3, if full adiabatic flame conditions are reached in the gas pocket formed from the liquid phase reactions, it only takes tens of microseconds to fully ignite the mixture. While the induction time for initiation of the explosive behavior is long in these tests, one might envision a much shorter time when smaller amounts of fluid are involved, i.e. the energy losses to the pool could extend the delay to realizing the explosive behavior.

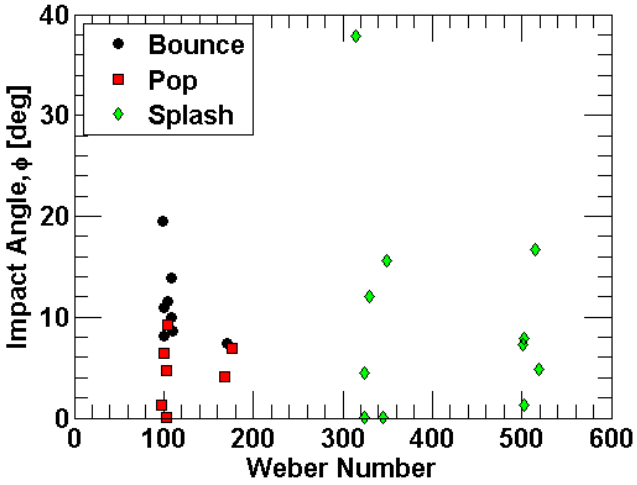


Figure 12: Classification of outcomes of drop/pool collisions in terms of Weber number and impact angle.

Gas evolution is highly apparent in the droplet collision processes as evidenced by the sequence of events in Figs. 9-11. Using image processing tools, Forness [2] has provided a quantitative determination of the velocity of expansion of these gases as they emanate from the collision region. Figure 13 provides a glimpse at these results, once again classified in terms of collision Weber number. To our knowledge, this is the first such determination of this gas generation/expansion rate and it provides an important criterion to support advanced spray combustion simulations. The results certainly show a chaotic behavior, but the order of magnitude is in the 1-10 m/s range, or 1000-10,000 μm/ms. For the collision of two 50 μm drops in a spray, these values imply that the entire droplet collision region will be enveloped in gases stemming from liquid phase reactions in fractions of a millisecond. Clearly these gas clouds provide a vital energy source for ignition in the dilute spray region and the competition between heating from these gases and energy losses to the surroundings provide the underlying criteria for ignition.

An important contribution of this research has been the measurement of the liquid phase, acid-base neutralization reaction time, which is believed to be the first step in hypergolic ignition. The delay measured was from first discernible propellant contact to first visible gas production. This delay contains information about the speed of the liquid-phase reactions, the heat produced by the reactions, as well as the time before gas-phase reactions begin to contribute. It is also a convenient metric to use to validate computer models of hypergolic contact, and has already been applied toward that end. The measurement was made in the drop contact chamber, at room temperature, atmospheric pressure, and in a quiescent nitrogen atmosphere. The propellants used were MMH/RFNA at room temperature (20°C). A Phantom v7.3 high-speed camera set to a resolution of 128 x 88 pixels, with an exposure of 8 μs and frame rate of 100,000 FPS was used to observe the impacts. The frame rate and resolution of the test were limited by the 3.0 Gpixels/s maximum throughput of the camera.

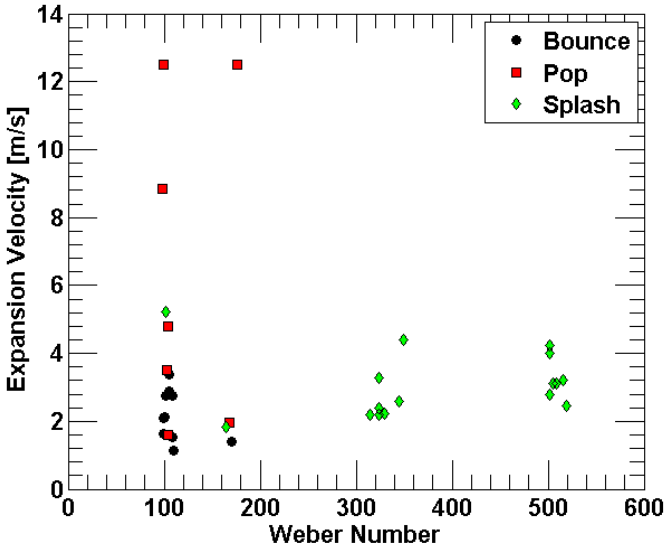


Figure 13: Average gas expansion velocities emanating from MMH drop colliding with WFNA pool.

Figure 14 shows a side-by-side comparison of the time of contact and gas production between a reactive test and one with non-reactive propellant simulants. Contact was taken to be the time when there was a disturbance in the drop shape, and gas production was taken as the time when the reactive test deviated from the contour of the simulant test. There was some ambiguity as to the precise moment of contact and first gas production. The gas production delay was measured to be no less than 20 μs with an average of 160 ± 50 μs. Gas is first observed in a jet emanating from the drop/pool interface. The velocity of the gas and secondary droplets in this jet was measured at 3 m/s, although somewhere in this interface, there must exist gas with enough velocity to shear off secondary droplets.

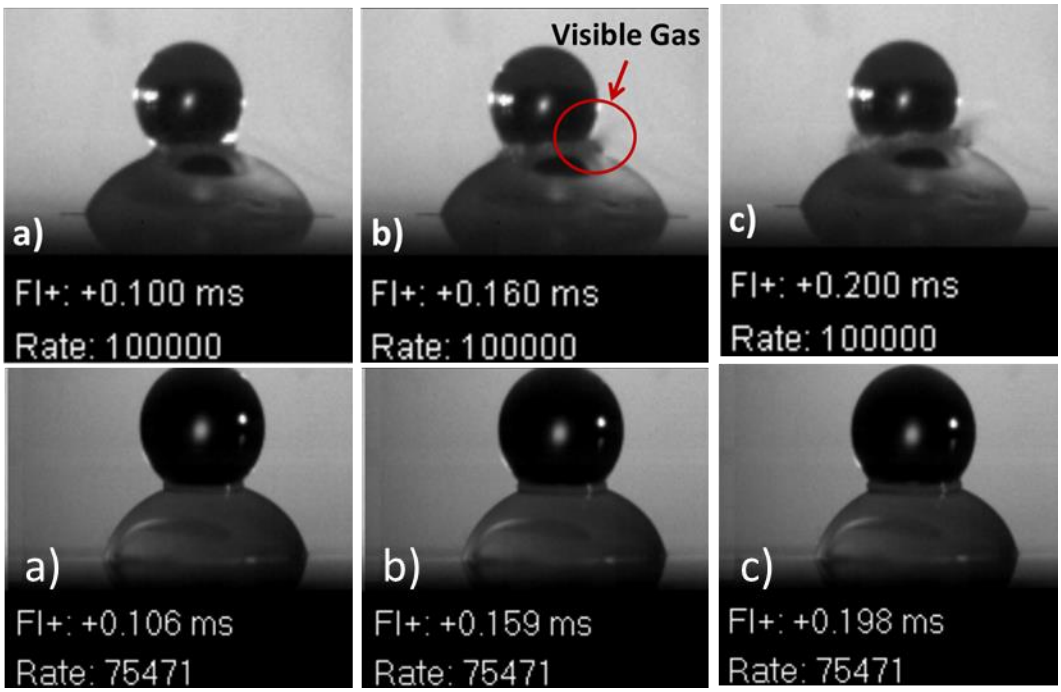


Figure 14: Comparison of an MMH/RFNA impact (Left column) with a water/water impact (Right Column). All times are referenced to contact. Both impact velocities are 1.3 m/s, (Left) d = 2.5 mm, We = 137, E = 13.9; (Right) d = 2.9 mm, We = 67, E = 10.0.

## Conclusions

Progress is being made in increasing our understanding of physical-chemical processes governing hypergolic ignition events. Modern chemical kinetics computations for RFNA/MMH propellants are uncovering the importance of liquid-phase reactions as a necessary precursor to ignition. Computations with modern kinetics reaction sets shows that temperatures of 550-650 K must be produced by these liquid phase reactions in order to bootstrap gas phase reactions to ignition within times typically observed in experiments. Since the liquid phase reactions are showing adiabatic decomposition temperature in excess of 1200 K there is ample energy available from this reaction mechanism.

Kinetics, heat transfer and hydrodynamics share important roles in the impact region between impinging jets. Gases generated from liquid phase reactions have been observed to appear as quickly as 20 microseconds from the impact event and serve to separate the propellants, but are subject to collapse via Rayleigh-Taylor instabilities. Temperatures generated from the reactions can be quickly quenched by the large enthalpy of liquid reactants in the region adjacent to thin films. Recent simulations are showing average gas film thicknesses of the order of 40 microns and residence times in the neighborhood of a few hundred microseconds.

Recent drop impact studies are revealing three distinct outcomes: explosions, bounces, and splashes. The impact type has been best correlated with impact Weber number and impact angle. Splashes occurred above a critical Weber number of 250, regardless of impact angle. Explosions occurred for Weber numbers less than 250, so long as the impact angle was less than seven degrees. If the impact angle was greater than seven degrees then a bounce resulted. Each impact type resulted in different gas production rates and different degrees of atomization; both of which would affect the ignitability of the mixture. It is postulated that the fluid dynamics of the impact created differences in the distribution of the fuel drop and produced the different impact types.

## References


[1]. T. L. Pourpoint and W. E. Anderson. Hypergolic reaction mechanisms of catalytically promoted fuels with rocket grade hydrogen peroxide. Combustion Science and Technology, 179(10):2107- 2133, 2007.

[2]. J. M. Forness. Phenomena resulting from hypergolic contact. MS thesis, Purdue University, West Lafayette, IN, August 2013.

[3]. T. F. Seamans and B. E. Dawson. Hypergolic ignition at reduced pressures. Technical Report AFRPL-TR-67-129. USAF Rocket Propulsion Laboratory, Edwards AFB, California, 1967.

[4]. Pourpoint T. L. Hypergolic ignition of a catalytically promoted fuel with rocket grade hydrogen peroxide. Phd thesis, Purdue University, ·west Lafayette, IN, December 2005.

[5]. W. E., Anderson, H. M., Ryan, and R. J., Santoro. A model for impinging jet atomization. CPIA Publication 629, Vol. II, Marshall Space Flight Center, AL, 1995.

[6]. W. A. Anderson, M. J. McQuaid, NI. J. Nusca, and A. J. Kotlar. A detailed, finite-rate chemical kinetics mechanism for monomethylhydrazine-red fuming nitric acid systems. Weapons and materials research directorate ARL-TR-5088, Army research laboratory, Aberdeen Proving Grounds, MD, 2010.

[7]. S. Sardeshmukh, S. Heister, G. Xia, C. Merkle. Kinetic modeling of hypergolic propellants using impinging element injectors. AIAA 2012-3760, 48th AIAA Joint Propulsion Conference, 2012.

[8]. J.E. Smith. Time resolved measurements and reactive pathways of hypergolic bipropellant combustion. Final Report DAAD19-02-1-0356, Army Research Office, 2006.

[9]. S.Q. Wang, S.T. Thynell. An experimental study on the hypergolic interaction between monomethylhydrazine and nitric acid. Combustion and Flame, Vol. 159, 2012.

[10]. N. Labbe, Y. Kim, and P. Westmoreland. “Mechanism Development for Hypergolic Propellant Systems: MMH and DMAZ.” Reaction Path Analysis I, 2010 AIChE National Meeting, Salt Lake City, UT, Nov. 2010

[11]. O.W. Jayaratne and B. J. Mason. The coalescence and bouncing of water drops at an air/water interface. Proc. Royal society of London A, 280, 1964.

[12]. E. M. Dambach, Y. Solomon, S. D. Heister, and T. L. Pourpoint. Investigation into the hypergolic ignition mechanisms initiated by low weber number collisions. J. Propulsion and Power, 29(2), 2013.